

Manuscript title: Hanging glacier monitoring with icequake repeaters and seismic coda wave interferometry: a case study of the Eiger hanging glacier

Manuscript ID: NHESS-2021-205

Response to Reviewer 2:

Review of "Hanging glacier monitoring with icequake repeaters and seismic coda wave interferometry: a case study of the Eiger hanging glacier" by Chmiel et al.

This is a paper examining seismic data collected on a hanging glacier during a time period containing a break-off event from the front of the glacier in 2016. The seismic data are interpreted along with temperature data, surface velocity of the glacier front, and remote cameras. I think the paper is worthy of publication and came away with these comments:

Our response: We thank the Reviewer for this helpful review and the important comments. Please find our responses to Reviewer's comments below. We provide our detailed responses to each Reviewer's comment below. The Reviewer's comments are marked in blue, our responses in black, and parts of the manuscript are marked in *italic*.

- Figure B1 shows an infrasound array, but there is no mention of those data in the paper. Has there been analysis of the infrasound data and did it show anything besides presumably the signal from the large break-off event?

Our response: Unfortunately, the infrasound array was not operational during the break off event. However, a recent study by Marchetti et al., (2021) shows the analysis of the infrasound signals from a break-off event that occurred at the Eiger hanging glacier on May 29, 2017, and the potential for infrasound records to provide quantitative information of glacier collapse and ice avalanche trajectories, and possibly, volume. We will add the following sentence to the manuscript:

- The authors mention at line 80 that up to 3 of the seismic stations operated simultaneously at times. Which made me wonder if any array method could be applied to the 3 stations during that time, using the 3 stations as a tripartite array? Such beamforming (like what is done with infrasound arrays) could complement the polarization analysis.

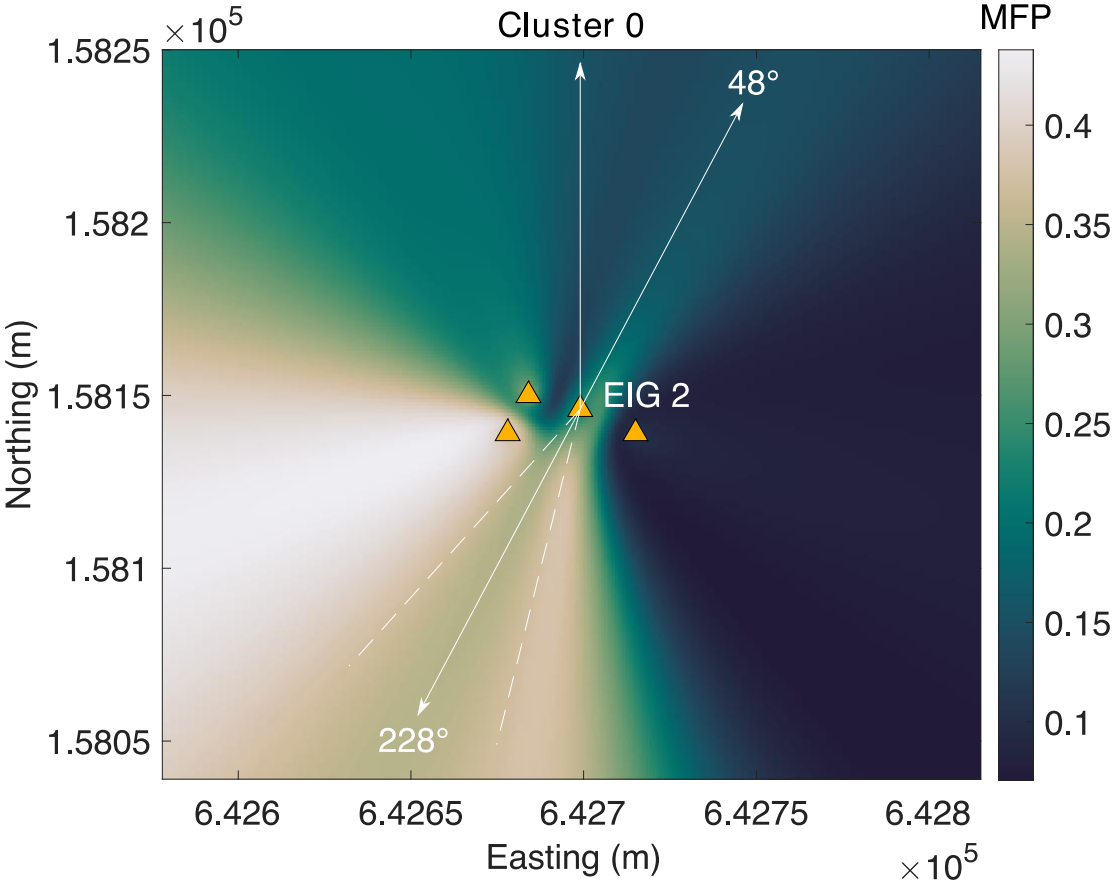
Our response: We thank the Reviewer for this very useful suggestion. We performed an additional beamforming analysis to resolve the 180° ambiguity in the polarization analysis. Also, following the remarks of the Reviewer 1 we now present more details of the backazimuth analysis.

We use Matched Field Processing (MFP, Baggeroer et al. 1988; Kuperman and Turek 1997) to locate the icequakes. MPF exploits cross-array signal coherence and this method is based on the calculation of the cross-spectral correlation matrix (CSDM, Kuperman and Turek 1997),

which represents the coherence of the wavefield recorded at a group of sensors. We do not go into technical details here, they can be found in Chmiel et al., 2019 and Bowden et al., 2021. We use both phase and amplitude information of the icequakes (Bowden et al., 2021) assuming a 2D medium with a Rayleigh wave velocity=1600 m/s.

The four stations were never in operation simultaneously, therefore for each cluster, and each station, we stack icequake waveforms recorded on the vertical component of the stations for time periods when the station was working properly. This provides us with average icequake waveform stacks for four stations. The value of the MFP is normalized in between 0 and 1 due to the normalization of the CSDM and model vector. We note though that the backazimuth estimates are obtained from the first arrivals, while MFP uses the entire icequake waveform (0-1.5s time window) assuming a 2-D Rayleigh wave propagation. This might cause a difference between the dominant backazimuth directions obtained from the two methods. We will add this analysis to the Appendix. Since the beamforming analysis is based on four stations it potentially yields more robust results compared to the single-station polarization analysis. In the revised manuscript, we will leverage the results of the two techniques to provide the most robust estimates of the backazimuth direction.

Please find below the result of the MFP for cluster 0:



18 Figure R1: MFP results for cluster 0 and the estimated backazimuth (including the 180°

ambiguity) with its uncertainty (marked in white dashed lines) obtained from the polarization analysis. MFP allows us to resolve the 180° ambiguity in the backazimuth estimates.

- In Appendix A5 the authors point out that the seismometers moved on the order of 1 meter during the deployment, which they argue does not affect their interpretation of the coda wave interferometry measurements. However, did the seismometers also happen to rotate at all in addition to the 1 meter of movement? Any rotation of the horizontal components could have an effect on the polarization analysis.

Our response: We thank the Reviewer for this comment. We agree that the rotation of the seismometers would affect the polarization analysis. However, the stations remained horizontal on the granite plate with no significant rotation. The stations were snow covered: they were initially buried in the 1-2 m trenches and subsequently covered under ~1-2m of snow, which might have prevented them from turning. We will add this information to the manuscript.

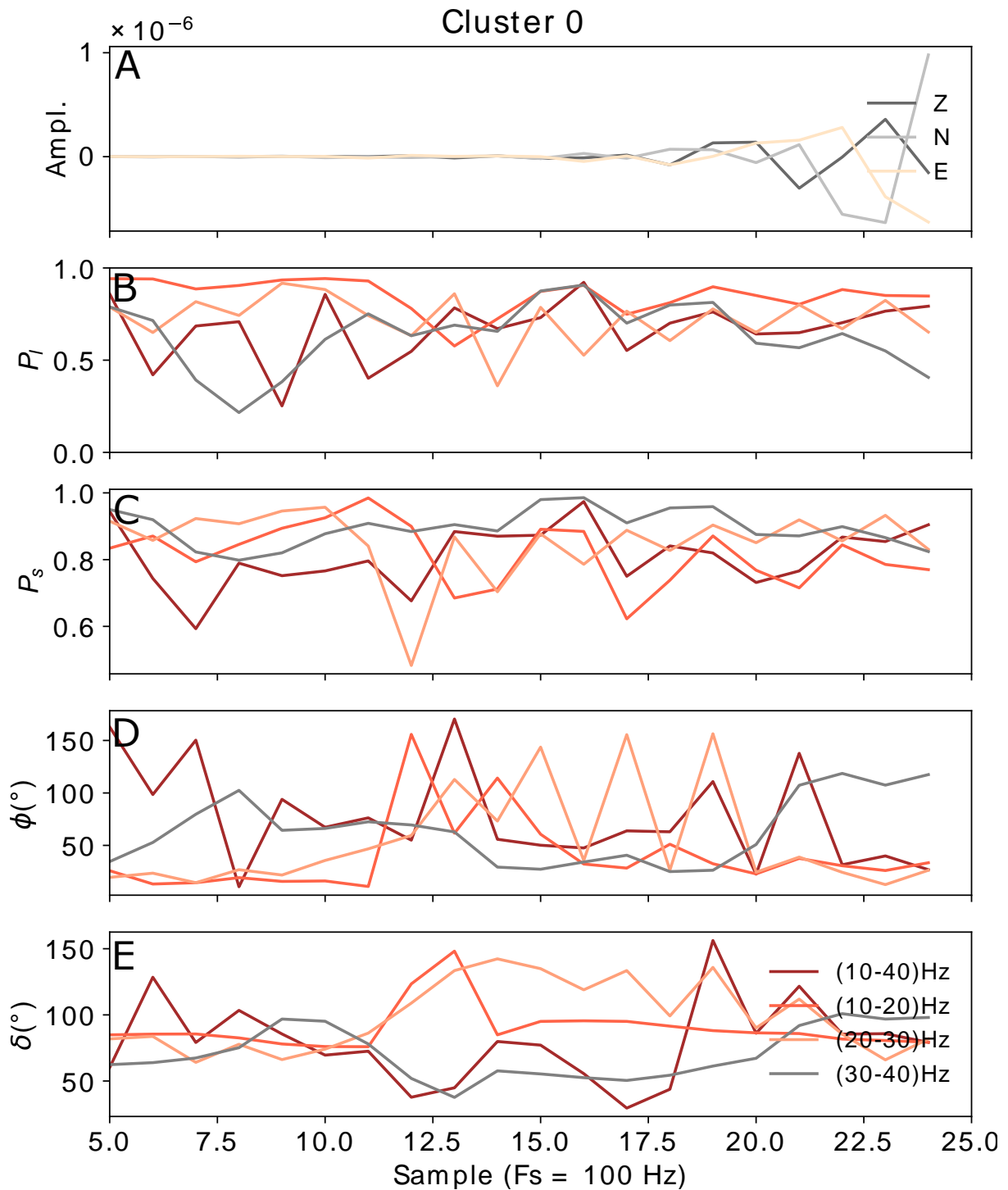
- Regarding the polarization analysis, was the same frequency bandpass used for it as was used for the coda wave interferometry (10-40 Hz)? What if there was significant frequency-dependency of the polarization over the band used? Have the authors looked at polarization in bandpassed data (e.g., 10-20 Hz, 20-30 Hz, 30-40 Hz) to see if the polarization is consistent as a function of frequency?

Our response: We initially performed the polarization analysis on the raw data. We verified that the results are mostly coherent for the raw data and (10-40) Hz filtered data. However, to keep the consistency between different analysis method, we will use the results from (10-40) Hz in the final manuscript.

Following the Reviewer suggestion, we investigated the polarization analysis in different frequency bands: (10-40), (10-20) Hz, (20-30) Hz, (30-40) Hz. In the final manuscript, we will show the results in (10-40) Hz for the consistency with the beamforming analysis.

Changes for different frequencies can be related to the dominance of different seismic phases in different frequency bands (surface waves over body waves), and changing sensitivity of analysis due to a use of a fixed time window. However, by consequently choosing time windows for which the polarization strength is > 0.9 and that correspond to the highest linear polarization, our analysis yields coherent results for cluster 0 (Table 1 and Figure R2).

Finally, we will calculate the final backazimuth values as medians over frequency bands: (10-40), (10-20), (20-30), (30-40) Hz and we will provide uncertainty of the backazimuth estimates taken as a standard deviation of the estimated backazimuth values in four different frequency bands. We will add this information to the appendix.



4 Figure R2: Polarization analysis for cluster 0 (limited to the time window containing the first
 6 arrivals) in four different frequency bands: (10-40), (10-20) Hz, (20-30) Hz, (30-40) Hz. A.
 Raw waveforms recorded over Z, N, and E, component. B. linearity, C. the strength of the
 polarization, D. estimated backazimuth, and E. dip as a function of time.

	Backazimuth(°)	Dip(°)
(10-40) Hz	48	56
(10-20) Hz	16	76
(20-30) Hz	22	66
(30-40) Hz	34	53
Mean	30	63
Median	28	61
Std	14	10
Raw	45	86

Table 1: Backazimuth and dip estimates in different frequency bands for cluster 0.

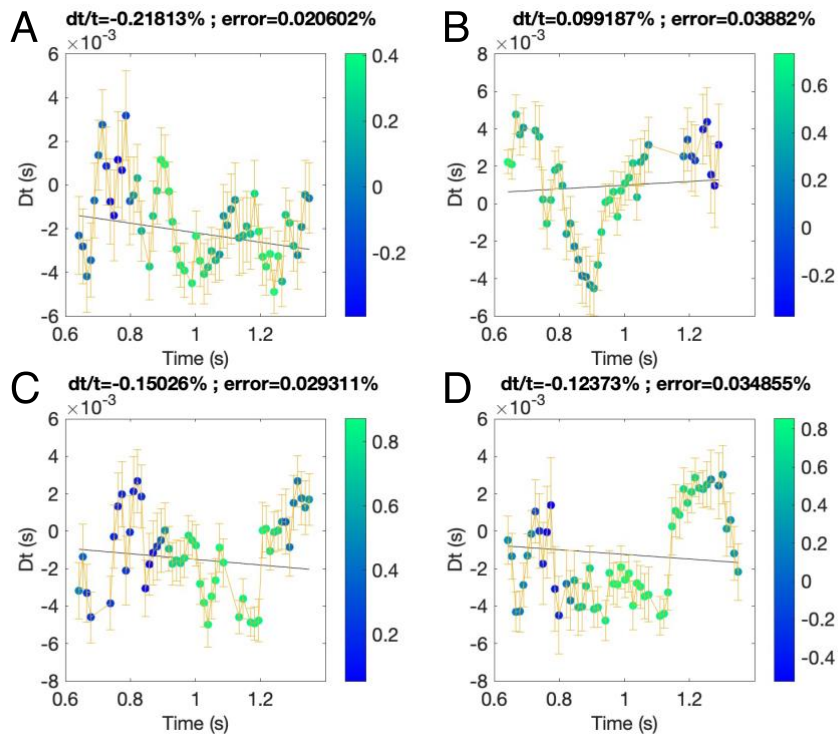
2 - I hate to say it, but I wasn't that impressed by the amount of fit in the dt/t plots in Figure A7.
4 I normally like to see much better of a linear fit in this type of plot. Are the ones shown in this
6 figure typical? What could be causing the significant lack of a linear trend in these plots? Have
8 the authors tried different approaches to defining the reference event? I wonder if there could
be an improvement by not even having a reference event and just measuring dt/t between all
the events and inverting for a continuous function of dv/v , as was done by Hotovec-Ellis et al.
(2014, JGR; 2015, JGR). I think that approach is sometimes referred to as the "all doublet"
method.

10 **Our response:** The dt/t plots shown in Figure A7 are rather typical in our analysis. We agree
12 with the Reviewer that the fit is not impressive, although, it must be noted that these
14 measurements are made on a glacier, where scattering is still strongly limited compared to
volcanic settings or crustal settings where CWI is commonly used. Moreover, the lack of linear
16 trend can be related to a localized perturbation in the glacier. Finally, the monochromatic coda
visible for certain icequakes (Figures A3 and A5 in the manuscript) and source displacement
of 0.3λ - 0.4λ (see the comments of the Reviewer 1) can cause cycle skipping that would be
18 visible as deviations in individual dt measurements. However, averaging dv/v measurements
over 69 individual measurements makes it statistically more representative and makes the
estimation of final dv/v variations robust.

20 And a small correction: Figure A7 in the manuscript showed the results for the dt/t
22 measurement for cluster 2, component E, not for cluster 0, component Z as stated in the
manuscript. We will correct the Figure caption in the new revised manuscript.

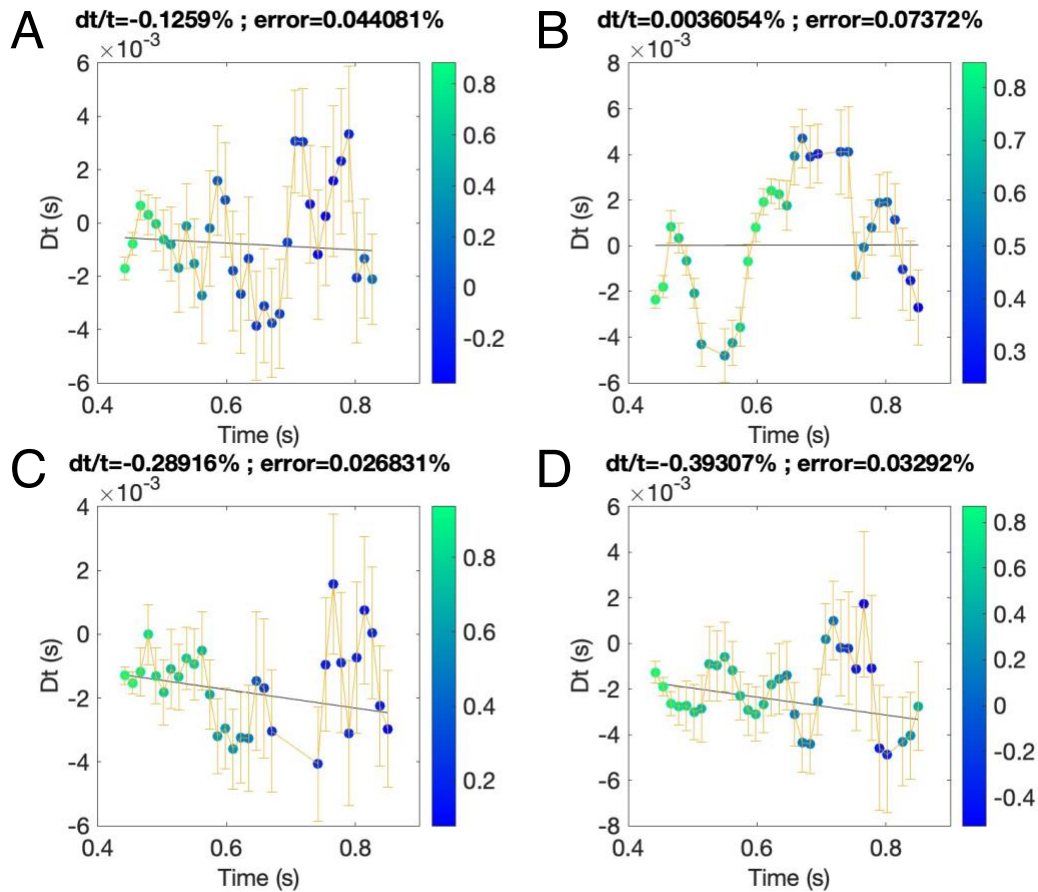
We performed different tests to verify our results:

24 1) We increased the overlap from 80% to 96% in measured time windows to add more
26 measurement point in the linear regression (Figure R3). We also reject individual dt
measurements if $dt > 0.005s$ or error of $dt > 0.005 s$.



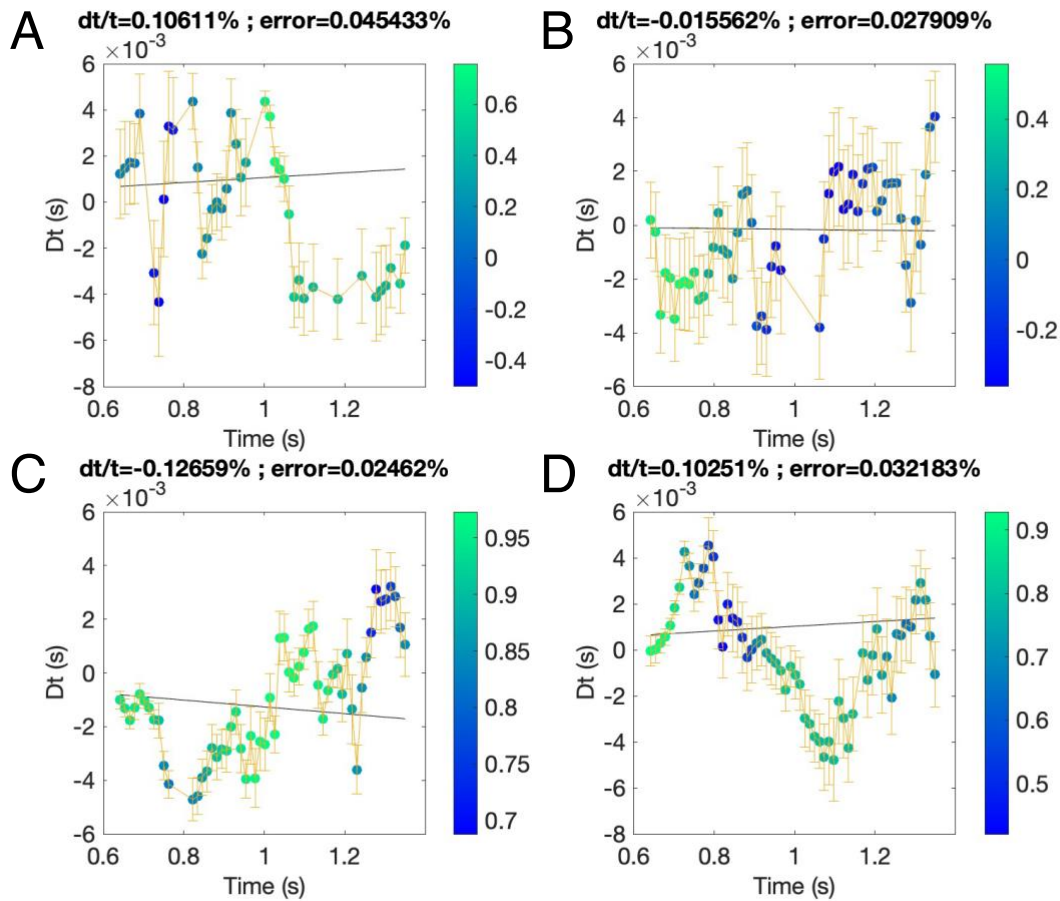
2 Figure R3: Examples of dt/t measurement using cross-correlation on sliding time windows and
 4 linear regression for cluster 2, component E. Cross-correlation between the reference and
 analysed signals for each time windows is presented in color, dt measurements in individual
 time windows with their error bars, at four dates: April 25, 2016, 20:00, (B) May 25, 2016,
 6 15:00, (C) August 12, 2016, 19:00, and (D) August, 2016, 19:00 (with an overlap of 96%).

2) We adjusted the coda time window for 0.3-1s with an overlap of 96% (Figure R4). We
 8 also reject individual dt measurements if $dt > 0.005$ s or error of $dt > 0.005$ s. This gives
 a better fit of the individual dt measurements.



2 Figure R4 Examples of dt/t measurement using cross-correlation on sliding time windows and
 4 linear regression for cluster 2, component E using coda in 0.3-1s time window. Cross-
 correlation between the reference and analysed signals for each time windows is presented in
 6 color, dt measurements in individual time windows with their error bars, at four dates: April
 25, 2016, 20:00, (B) May 25, 2016, 15:00, (C) August 12, 2016, 19:00, and (D) August, 2016,
 19:00 (with an overlap of 96%).

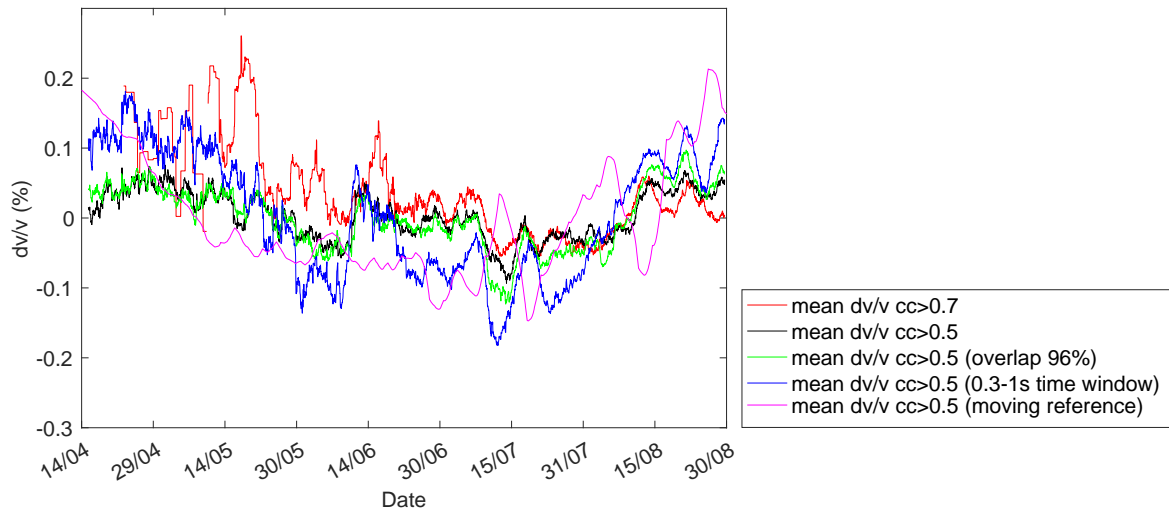
8 3) We tried also a moving reference approach as proposed by James et al., 2017. As a
 moving reference: we use the adjacent 3-day stack three days prior to the current day's
 10 stack. We also reject individual dt measurements if $dt > 0.005$ s or error of $dt > 0.005$ s.
 Then, to track the full velocity we cumulated the individual dv/v values. This approach
 12 does not significantly improve individual dt measurements and results in a linear drift
 caused by the error accumulation (James et al., 2017). We detrend the cumulative
 14 measurements to remove the linear drift due to the error accumulation. Note, that this
 might influence the accuracy of the results if there is a linear trend present in the dv/v
 16 measurements.



2 Figure R5: Examples of dt/t measurement using cross-correlation on sliding time windows and
 4 linear regression for cluster 2, component E using a moving reference. Cross-correlation
 6 between the reference and analysed signals for each time windows is presented in color, dt
 8 measurements in individual time windows with their error bars, at four dates: April 25, 2016,
 20:00, (B) May 25, 2016, 15:00, (C) August 12, 2016, 19:00, and (D) August, 2016, 19:00
 (with an overlap of 96%). These measurements are not the same as measurements in Figure R3
 and R4 due to the use of a moving reference, and the determined trends require a summation
 to contribute to the overall dv/v measurements shown in R6.

10 4) We also test dv/v measurements using only icequakes that were detected in template
 matching with a cross-correlation coefficient >0.7

12 The final results of the above tests show the same long-term variations as our initial results that
 increases our confidence that the estimates of final dv/v shown in the manuscript were robust.
 14 We will add a summary of this discussion and the references indicated by the Reviewer to the
 Appendix.



2 Figure R6: Dv/v results from different approaches described above. The dv/v results obtained
 with a moving reference were scaled ($dv/v/3$) for the purpose of visual comparison.

4 - In research papers over the past decade, I don't often see the measurement of coda-Q but I
 appreciated it in this paper. How do the authors decide which portion of the event to measure
 6 the Q_c on as shown in Fig. A6B?

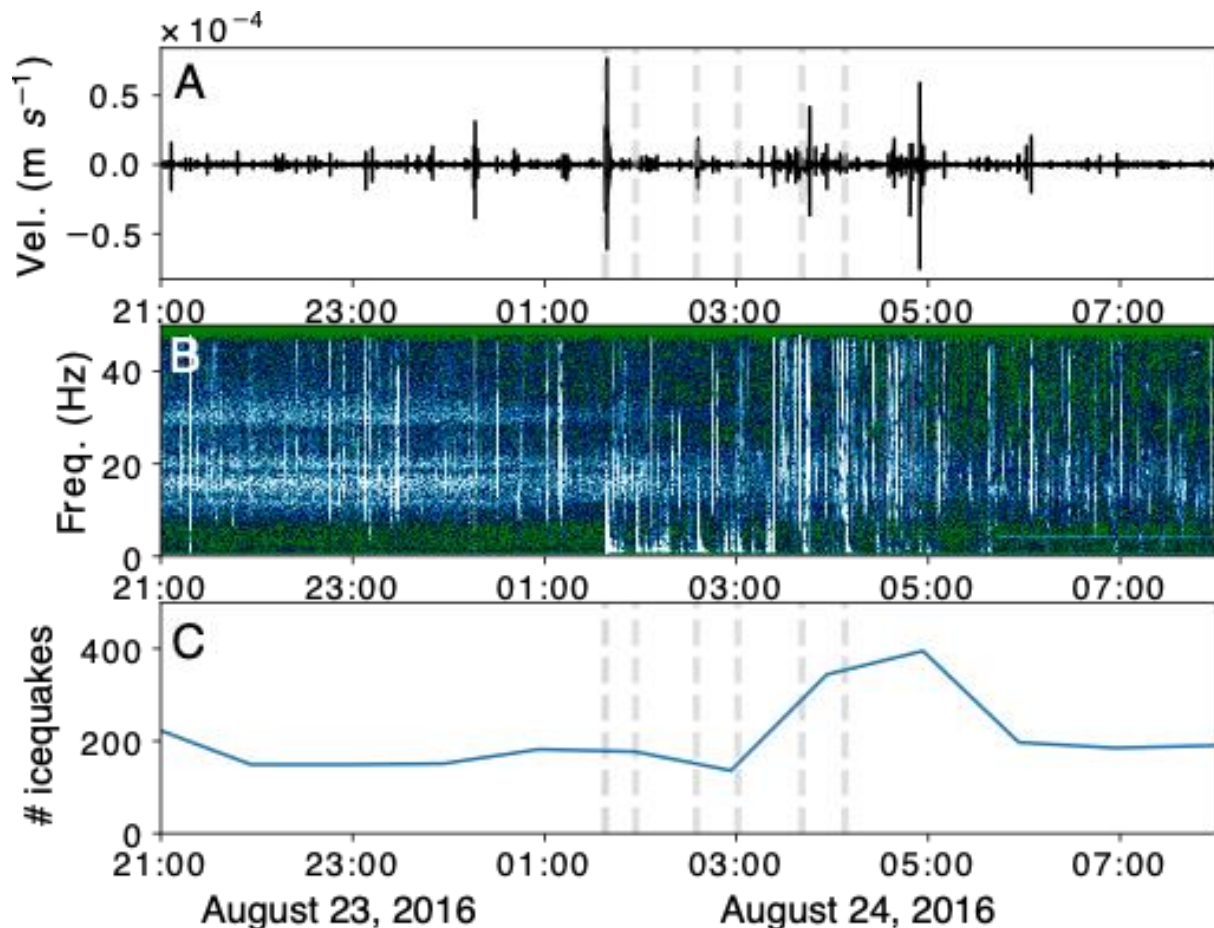
Our response: We thank the Reviewer for this comment. We chose the portion of the time
 8 windows arbitrarily by choosing as the beginning the time where the envelope of the seismic
 signal starts to decay in a regular, linear manner (Aki and Chouet, 1975) and as the end, the
 10 time where the envelope falls below the background noise levels (visible from 1.5s). We will
 add this information to the manuscript.

12 - The authors mention briefly that a period of increased seismicity correlated with the passage
 of a regional M6.2 earthquake in Fig. 1C. Have the authors looked in detail to see if increased
 14 icequake activity is in fact triggered by the regional earthquake? Or is the increased event rate
 due to distant aftershocks that are not local?

16
Our response: Thank you for this comment. We looked in detail into the icequake activity.
 18 The rate of icequake activity a few days before and after the earthquake is shown in Figure 1A
 in the manuscript and a few hours before and after the earthquake is shown in Figure R7 in this
 20 rebuttal letter. In the revised manuscript, we will also add the rate of cluster activity to the panel
 C in Figure R7.

22 Since remote triggering usually occurs during the passage of teleseismic surface waves, not
 several hours later, we did not want to suggest that this burst of the seismic activity was
 24 triggered by the Amartice earthquake. We will clarify this misunderstanding in the revised
 manuscript.

26



2 Figure R7: The rate of icequake activity for a few days before and after the M6.2 Amatrice
 4 earthquake. A. Vertical ground velocity recorded at the EIG2 station, B. the corresponding
 6 spectrogram, C. icequake activity between 21:00 August 23 and 08:00 August 24, 2016. The
 main shock and the aftershocks are shown in dashed gray lines (M6.2, M5.5, M4.6, M4.3,
 M4.3, M4.4).

Citation: <https://doi.org/10.5194/nhess-2021-205-RC2>

8

References

10 Aki, K. and Chouet, B.: Origin of coda waves: source, attenuation, and scattering effects, *Journal of geophysical*
research, 80, 3322–3342, 1975.

12

14 Baggeroer, A. B., Kuperman, W. A. and Schmidt, H., Matched field processing: Source localization in
 correlated noise as an optimum parameter estimation problem, *J. of the Acoustical Soc. of Amer.*, vol. 83, no.
 2, pp. 571-587, 1988.

16

18 Bowden, D.C, Sager, K., Fichtner, A., Chmiel, M., Connecting beamforming and kernel-based noise source
 inversion, *Geophysical Journal International*, 224, 3, 2021, 1607–1620, <https://doi.org/10.1093/gji/ggaa539>

20 Chmiel, M., Roux, P., Bardainne, T.; High-sensitivity microseismic monitoring: Automatic detection and
 localization of subsurface noise sources using matched-field processing and dense patch arrays. *Geophysics* 2019;;
 22 84 (6): KS211–KS223. doi: <https://doi.org/10.1190/geo2018-0537.1>

2 James, S. R., H. A. Knox, R. E. Abbott, and E. J. Sreaton (2017), Improved moving window cross-spectral
analysis for resolving large temporal seismic velocity changes in permafrost, *Geophys. Res. Lett.*, 44, 4018–
4026, doi:10.1002/2016GL072468.

4

Kuperman, W.A., Turek, G., 1997. Matched field acoustics, *Mech. Syst. Signal Process.*, 11, 141–148

6

Marchetti, E., Walter, F., & Meier, L. (2021). Broadband infrasound signal of a collapsing hanging glacier.

8

Geophysical Research Letters, 48, e2021GL093579. <https://doi.org/10.1029/2021GL093579>